

Dust-ion-acoustic rogue waves in dusty plasma having super-thermal electrons

A.A. Noman^{1,*}, M.K. Islam^{1,**}, M. Hassan^{1,***}, S. Banik^{1,2,†}, N.A. Chowdhury^{3,‡}, A. Mannan^{1,4,§}, and A.A. Mamun^{1,§§}

¹ Department of Physics, Jahangirnagar University, Savar, Dhaka-1342, Bangladesh

² Health Physics Division, Atomic Energy Centre, Dhaka-1000, Bangladesh

³ Plasma Physics Division, Atomic Energy Centre, Dhaka-1000, Bangladesh

⁴ Institut für Mathematik, Martin Luther Universität Halle-Wittenberg, 06009 Halle, Germany

e-mail: *noman179physics@gmail.com, **islam.stu2018@juniv.edu, ***hassan206phy@gmail.com, †bsubrata.37@gmail.com

‡nurealam1743phy@gmail.com, §abdulmannan@juniv.edu, §§mamun_phys@juniv.edu

Abstract

The standard nonlinear Schrödinger equation (NLSE) is one of the elegant equations to find the information about the modulational instability criteria of dust-ion-acoustic (DIA) waves (DIAWs) and associated DIA rogue waves (DIARWs) in a three-component dusty plasma medium having inertialess super-thermal kappa distributed electrons, and inertial warm positive ions and negative dust grains. It can be seen that under the consideration of inertial warm ions along with inertial negatively charged dust grains, the plasma system supports both fast and slow DIA modes. The charge state and number density of the ion and dust grain are responsible to change the instability conditions of the DIAWs and the configuration of DIARWs. These results are to be considered the cornerstone for explaining the real puzzles in space and laboratory dusty plasmas.

Keywords: Dust-ion-acoustic waves; modulational instability; rogue waves

1. Introduction

The size, mass, charge and ubiquitous existence of massive dust grains in both space (viz., cometary tails [1, 2, 3, 4], magnetosphere [3], ionosphere [3], aerosols in the astrosphere [2, 4], planetary rings [1], Earth's ionospheres [1], nebula, and interstellar medium [4], etc.) and laboratory (viz., ac-discharge, plasma crystal [4], Q-machine, nano-materials [5], and rf-discharges [4], etc.) plasmas do not only change the dynamics of the dusty plasma medium (DPM) but also change the mechanism of the formation of various nonlinear electrostatic excitations, viz., dust-acoustic (DA) solitary waves (DASWs) [6], DA shock waves (DA-SHWs) [7], dust-ion-acoustic (DIA) solitary waves (DIASWs) [1, 2, 3], DIA shock waves (DIASHWs), and DIA rogue waves (DIARWs), etc.

The activation of the long range gravitational and Coulomb force fields is the main cause to generate non-equilibrium species [8] as well as the high energy tail in space environments, viz., terrestrial plasma-sheet [9, 10], magneto-sheet, auroral zones [9, 10], mesosphere, radiation belts [9, 10], magnetosphere, and ionosphere [9, 10], etc. The Maxwellian velocity distribution function, in which the dynamics of the non-equilibrium species is not considered, is not enough to describe the intrinsic mechanism of the high energy tail in space environments [8]. While the super-thermal/ κ -distribution function, in which the dynamics of the non-equilibrium species is also considered, is suitable for explaining the high energy tail in space environments [8]. The non-equilibrium properties of the species are recognized by the magnitude of κ in super-thermal κ -distribution [8]. The κ -distribution is normalizable for a range of values of κ from $\kappa > 3/2$ to $\kappa \rightarrow \infty$, and the non-equilibrium

properties of the species is considerable when the value of κ tends to $3/2$ [1, 2, 3, 8]. Eslami *et al.* [1] observed that the velocity of the DIASWs increases with decreasing the value of κ in DPM. Shahmansouri and Tribeche [3] considered an electron depleted DPM having super-thermal plasma species to investigate DASWs, and reported that the amplitude of the DASWs increases while the width of the DASWs decreases with a decrease in the value of κ that means the super-thermality of the plasma species leads a narrower and spiky solitons. Ferdousi *et al.* [7] numerically observed that the height of the positive DASHWs increases while negative DASHWs decreases with increasing the value of κ in a multi-component DPM in the presence of super-thermal electrons.

The nonlinear and dispersive properties of plasma medium are the prime reasons to organize the modulational instability (MI) criteria of various kinds of waves in the presence of external perturbation, and are governed by the standard nonlinear Schrödinger equation (NLSE) which can be derived by employing reductive perturbation method (RPM) [11, 12, 13, 14, 15, 16, 17, 18, 19]. The rational solution of the NLSE is also known as freak waves, giant waves, or rogue waves (RWs) in which a large amount of energy can concentrate into a small area, and the height of the RWs is almost three times greater than the height of associated normal carrier waves. Initially, RWs are identified only in the ocean and are considered as a destructive sign of nature which can sink the ship or destroy the house in the bank of the ocean. Now-a-days, RWs can also be observed in optics, stock market, biology, and plasma physics, etc. Gill *et al.* [6] investigated the MI of the DAWs in a multi-component DPM and found that the critical wave number (k_c)

which defines the modulationally stable and unstable parametric regimes decreases with the increase in the value of κ . Amin *et al.* [11] studied the propagation of nonlinear electrostatic DAWs and DIAWs, and their MI in a three-component DPM. Jukui and He [12] demonstrated the amplitude modulation of spherical and cylindrical DIAWs. Saini and Kourakis [13] considered a three-component DPM having inertial highly charged massive dust grains and inertialess electrons and ions to study the MI of DAWs, and highlighted that the angular frequency of the DAWs increases with the super-thermality of the plasma species and the stable parametric regime decreases with an increase in the value of negative dust number density.

The outline of the paper is as follows: The governing equations describing our plasma model are presented in section 2. The derivation of NLSE is demonstrated in section 3. The Modulational instability and rogue waves is described in section 4. Results and discussion are devoted in section 5. Conclusion is provided in section 6.

2. Governing Equations

We consider an unmagnetized, fully ionized and collisionless three-component DPM comprising super-thermal electrons, positively charged inertial warm ions and negatively charged dust grains. At equilibrium, the overall charge neutrality conditions of our plasma system can be written as $n_{e0} + Z_d n_{d0} = Z_i n_{i0}$, where n_{e0} , n_{d0} , and n_{i0} are the equilibrium electron, dust, and ion number densities respectively, and Z_d (Z_i) is the charge state of the negative (positive) dust grain (ion). The normalized equations describing the system can be written as

$$\frac{\partial n_d}{\partial t} + \frac{\partial}{\partial x}(n_d u_d) = 0, \quad (1)$$

$$\frac{\partial u_d}{\partial t} + u_d \frac{\partial u_d}{\partial x} = \mu_1 \frac{\partial \phi}{\partial x}, \quad (2)$$

$$\frac{\partial n_i}{\partial t} + \frac{\partial}{\partial x}(n_i u_i) = 0, \quad (3)$$

$$\frac{\partial u_i}{\partial t} + u_i \frac{\partial u_i}{\partial x} + \mu_2 n_i \frac{\partial n_i}{\partial x} = -\frac{\partial \phi}{\partial x}, \quad (4)$$

$$\frac{\partial^2 \phi}{\partial x^2} + n_i = (1 - \mu_3)n_e + \mu_3 n_d, \quad (5)$$

where n_d (n_i) is the dust (ion) number density normalized by the equilibrium value n_{d0} (n_{i0}); u_d (u_i) is the dust (ion) fluid speed normalized by the ion sound speed $C_i = (Z_i k_B T_e / m_i)^{1/2}$ (where T_e being the super-thermal electron temperature, m_i is the ion rest mass, and k_B is the Boltzmann constant); ϕ is the electrostatic wave potential normalized by $k_B T_e / e$ (with e being the electron charge). The time variable t is normalized by $\omega_{p_i}^{-1} = [m_i / (4\pi e^2 Z_i^2 n_{i0})]^{1/2}$ and the space variable x is normalized by $\lambda_{D_i} = (k_B T_e / 4\pi e^2 Z_i n_{i0})^{1/2}$. The pressure of the ion is expressed as $P_i = P_{i0} (N_i / N_{i0})^\gamma$, where $P_{i0} = n_{i0} k_B T_i$ being the equilibrium pressure of the ion, and T_i being the warm ion temperature, and $\gamma = (N + 2) / N$ (where N be the degree of freedom and for one dimensional case $N = 1$, then $\gamma = 3$). Other plasma parameters are defined as $\mu_1 = \rho \mu$, $\rho = Z_d / Z_i$, $\mu = m_i / m_d$, $\mu_2 = 3T_i / Z_i T_e$, and $\mu_3 = Z_d n_{d0} / Z_i n_{i0}$. The expression for the number density

of the super-thermal electrons (following the κ -distribution) can be expressed as

$$n_e = \left[1 - \frac{\phi}{\kappa - 3/2} \right]^{-\kappa + \frac{1}{2}} = 1 + n_1 \phi + n_2 \phi^2 + n_3 \phi^3 + \dots, \quad (6)$$

where $n_1 = (2\kappa - 1) / (2\kappa - 3)$, $n_2 = [(2\kappa - 1)(2\kappa + 1)] / 2(2\kappa - 3)^2$, and $n_3 = [(2\kappa - 1)(2\kappa + 1)(2\kappa + 3)] / 6(2\kappa - 3)^3$. The parameter κ , generally stands for super-thermality, which measures the deviation of the plasma particles from Maxwellian distribution. Now, by substituting Eq. (6) into (5) and expanding up to third order in ϕ , we get

$$\frac{\partial^2 \phi}{\partial x^2} + n_i + \mu_3 = 1 + \mu_3 n_d + A_1 \phi + A_2 \phi^2 + A_3 \phi^3 + \dots, \quad (7)$$

where $A_1 = n_1(1 - \mu_3)$, $A_2 = n_2(1 - \mu_3)$, and $A_3 = n_3(1 - \mu_3)$.

3. Derivation of the NLSE

To study the MI of the DIAWs, we want to derive the NLSE by employing the RPM. First, we can write the stretched coordinates in the following form [20, 21, 22, 23, 24]

$$\xi = \epsilon(x - v_g t), \quad (8)$$

$$\tau = \epsilon^2 t, \quad (9)$$

where v_g is the group velocity and ϵ ($0 < \epsilon < 1$) is a small parameter. We can write the dependent variables (n_d , u_d , n_i , u_i , and ϕ) as

$$n_d = 1 + \sum_{m=1}^{\infty} \epsilon^m \sum_{l=-\infty}^{\infty} n_{dl}^{(m)}(\xi, \tau) e^{il(kx - \omega t)}, \quad (10)$$

$$u_d = \sum_{m=1}^{\infty} \epsilon^m \sum_{l=-\infty}^{\infty} u_{dl}^{(m)}(\xi, \tau) e^{il(kx - \omega t)}, \quad (11)$$

$$n_i = 1 + \sum_{m=1}^{\infty} \epsilon^m \sum_{l=-\infty}^{\infty} n_{il}^{(m)}(\xi, \tau) e^{il(kx - \omega t)}, \quad (12)$$

$$u_i = \sum_{m=1}^{\infty} \epsilon^m \sum_{l=-\infty}^{\infty} u_{il}^{(m)}(\xi, \tau) e^{il(kx - \omega t)}, \quad (13)$$

$$\phi = \sum_{m=1}^{\infty} \epsilon^m \sum_{l=-\infty}^{\infty} \phi_l^{(m)}(\xi, \tau) e^{il(kx - \omega t)}, \quad (14)$$

where k and ω are the real variables representing the carrier wave number and frequency, respectively. The derivative operators can be written as

$$\frac{\partial}{\partial x} \rightarrow \frac{\partial}{\partial x} + \epsilon \frac{\partial}{\partial \xi}, \quad (15)$$

$$\frac{\partial}{\partial t} \rightarrow \frac{\partial}{\partial t} - \epsilon v_g \frac{\partial}{\partial \xi} + \epsilon^2 \frac{\partial}{\partial \tau}. \quad (16)$$

Now, by substituting Eqs. (8)-(16) into Eqs. (1)-(4), and (7), and collecting the terms containing ϵ , the first order ($m = 1$

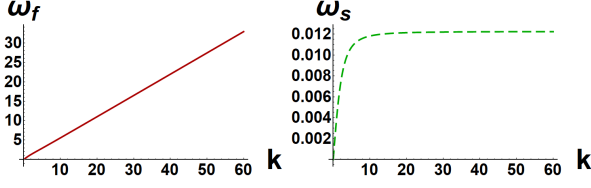


Figure 1: The variation of ω_f vs k (left panel) and ω_s vs k (right panel) when other plasma parameters are $\kappa = 1.8$, $\rho = 1 \times 10^3$, $\mu = 3 \times 10^{-6}$, $\mu_2 = 0.3$, and $\mu_3 = 0.05$.

with $l = 1$) reduced equations can be written as

$$u_{d1}^{(1)} = -\frac{k\mu_1}{\omega}\phi_1^{(1)}, \quad (17)$$

$$n_{d1}^{(1)} = -\frac{\mu_1 k^2}{\omega^2}\phi_1^{(1)}, \quad (18)$$

$$u_{i1}^{(1)} = -\frac{k\omega}{\mu_2 k^2 - \omega^2}\phi_1^{(1)}, \quad (19)$$

$$n_{i1}^{(1)} = -\frac{k^2}{\mu_2 k^2 - \omega^2}\phi_1^{(1)}, \quad (20)$$

these relations provide the dispersion relations of DIAWs. Now, the dispersion relations of DIAWs are

$$\omega^2 \equiv \omega_f^2 = \frac{k^2 M + k^2 \sqrt{M^2 - 4GH}}{2G}, \quad (21)$$

and

$$\omega^2 \equiv \omega_s^2 = \frac{k^2 M - k^2 \sqrt{M^2 - 4GH}}{2G}, \quad (22)$$

where $M = 1 + \mu_1 \mu_3 + \mu_2 k^2 + A_1 \mu_2$, $G = A_1 + k^2$, and $H = \mu_1 \mu_2 \mu_3$. In Eqs. (21) and (22), to get the positive value of ω , the condition $M^2 > 4GH$ must be satisfied. In the fast (ω_f) DIA mode, both inertial ion and dust oscillate in phase with the inertialess electrons. While in the slow (ω_s) DIA mode, one of the inertial elements ion (dust) oscillates in phase with the inertialess electrons and other inertial element dust (ion) oscillates in anti-phase with them [25, 26]. Both the fast (ω_f) and slow (ω_s) DIA modes have been analyzed numerically in Fig. 1 in the presence of super-thermal electrons. The second-order (when $m = 2$ with $l = 1$) equations are given by

$$u_{d1}^{(2)} = -\frac{k\mu_1}{\omega}\phi_1^{(2)} - \frac{\mu_1}{i\omega}\frac{\partial\phi_1^{(1)}}{\partial\xi} + \frac{kv_g\mu_1}{i\omega^2}\frac{\partial\phi_1^{(1)}}{\partial\xi}, \quad (23)$$

$$n_{d1}^{(2)} = -\frac{\mu_1 k^2}{\omega^2}\phi_1^{(2)} + \frac{2k\mu_1(kv_g - \omega)}{i\omega^3}\frac{\partial\phi_1^{(1)}}{\partial\xi}, \quad (24)$$

$$u_{i1}^{(2)} = \frac{k\omega}{\omega^2 - \mu_2 k^2}\phi_1^{(2)} - \frac{i(\omega - kv_g)(\omega^2 + \mu_2 k^2)}{(\omega^2 - \mu_2 k^2)^2}\frac{\partial\phi_1^{(1)}}{\partial\xi}, \quad (25)$$

$$n_{i1}^{(2)} = \frac{k^2}{\omega^2 - \mu_2 k^2}\phi_1^{(2)} - \frac{2ik\omega(\omega - kv_g)}{(\omega^2 - \mu_2 k^2)^2}\frac{\partial\phi_1^{(1)}}{\partial\xi}, \quad (26)$$

with the compatibility condition

$$v_g = \frac{2\mu_1 \mu_3 k \omega (\omega^2 - \mu_2 k^2)^2 + 2k\omega^5 - 2k\omega^3 (\omega^2 - \mu_2 k^2)^2}{2k^2 \mu_1 \mu_3 (\omega^2 - \mu_2 k^2)^2 + 2k^2 \omega^4}. \quad (27)$$

The coefficients of the ϵ when $m = 2$ with $l = 2$ provides the second-order harmonic amplitudes which are found to be proportional to $|\phi_1^{(1)}|^2$

$$u_{d2}^{(2)} = A_4 |\phi_1^{(1)}|^2, \quad (28)$$

$$n_{d2}^{(2)} = A_5 |\phi_1^{(1)}|^2, \quad (29)$$

$$u_{i2}^{(2)} = A_6 |\phi_1^{(1)}|^2, \quad (30)$$

$$n_{i2}^{(2)} = A_7 |\phi_1^{(1)}|^2, \quad (31)$$

$$\phi_2^{(2)} = A_8 |\phi_1^{(1)}|^2, \quad (32)$$

where

$$A_4 = \frac{k^3 \mu_1^2 - 2A_8 \mu_1 k \omega^2}{2\omega^3},$$

$$A_5 = \frac{3k^4 \mu_1^2 - 2A_8 \mu_1 k^2 \omega^2}{2\omega^4},$$

$$A_6 = -\frac{2A_8 k \omega (\mu_2 k^2 - \omega^2)^2 + 3\mu_2 \omega k^5 + k^3 \omega^3}{2(\mu_2 k^2 - \omega^2)^3},$$

$$A_7 = -\frac{2A_8 k^2 (\mu_2 k^2 - \omega^2)^2 + 3\omega^2 k^4 + \mu_2 k^6}{2(\mu_2 k^2 - \omega^2)^3},$$

$$A_8 = \frac{(2A_2 \omega^4 + 3\mu_1^2 \mu_3 k^4) + 3\omega^6 k^4 + \mu_2 k^6 \omega^4}{2\omega^2 [(k^2 \mu_1 \mu_3 - 4k^2 \omega^2 - A_1 \omega^2) - k^2 \omega^2 (\mu_2 k^2 - \omega^2)^{-1}]}. \quad (33)$$

When $m = 3$ with $l = 0$ and $m = 2$ with $l = 0$ lead to zeroth harmonic modes as follows

$$u_{d0}^{(2)} = A_9 |\phi_1^{(1)}|^2, \quad (33)$$

$$n_{d0}^{(2)} = A_{10} |\phi_1^{(1)}|^2, \quad (34)$$

$$u_{i0}^{(2)} = A_{11} |\phi_1^{(1)}|^2, \quad (35)$$

$$n_{i0}^{(2)} = A_{12} |\phi_1^{(1)}|^2, \quad (36)$$

$$\phi_0^{(2)} = A_{13} |\phi_1^{(1)}|^2, \quad (37)$$

where

$$A_9 = \frac{k^2 \mu_1^2 - \mu_1 \omega^2 A_{13}}{\omega^2 v_g},$$

$$A_{10} = \frac{2k^3 \mu_1^2 v_g + k^2 \mu_1^2 \omega - \mu_1 \omega^3 A_{13}}{v_g^2 \omega^3},$$

$$A_{11} = \frac{v_g^2 A_{13} (\omega^2 - \mu_2 k^2)^2 + 2\mu_2 \omega k^3 + \mu_2 k^4 v_g + k^2 \omega^2 v_g}{(\omega^2 - \mu_2 k^2)^2 (v_g^2 - \mu_2)},$$

$$A_{12} = \frac{A_{13} (\omega^2 - \mu_2 k^2)^2 + 2\omega k^3 v_g + \mu_2 k^4 + k^2 \omega^2}{(\omega^2 - \mu_2 k^2)^2 (v_g^2 - \mu_2)},$$

$$A_{13} = \frac{(\omega^2 - \mu_2 k^2)^2 \times F_1 - v_g^2 \omega^3 (2\omega k^3 v_g + \mu_2 k^4 + k^2 \omega^2)}{\omega^3 (\omega^2 - \mu_2 k^2)^2 [\mu_1 \mu_3 (v_g^2 - \mu_2) + v_g^2 - A_1 v_g^2 (v_g^2 - \mu_2)]},$$

where $F_1 = (v_g^2 - \mu_2)(2A_2 v_g^2 \omega^3 + 2k^3 \mu_1^2 \mu_3 v_g + k^2 \omega \mu_1^2 \mu_3)$. Finally, the third-order harmonic modes (when $m = 3$ and $l = 1$) and with the help of Eqs. (17)-(37), given a set of equations which can be reduced to the standard NLSE:

$$i\frac{\partial\Phi}{\partial\tau} + P\frac{\partial^2\Phi}{\partial\xi^2} + Q|\Phi|^2\Phi = 0, \quad (38)$$

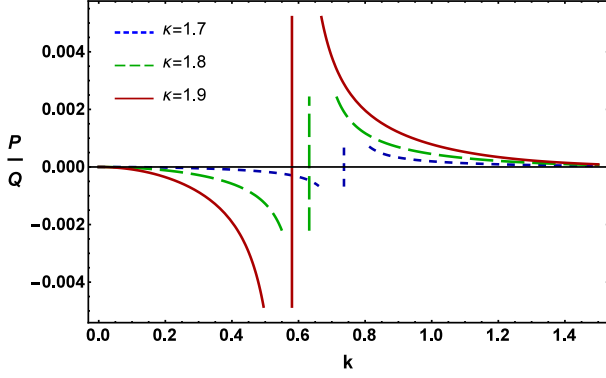


Figure 2: The variation of P/Q with k for different values of κ when other plasma parameters are $\rho = 1 \times 10^3$, $\mu = 3 \times 10^{-6}$, $\mu_2 = 0.3$, $\mu_3 = 0.05$, and $\omega \equiv \omega_f$.

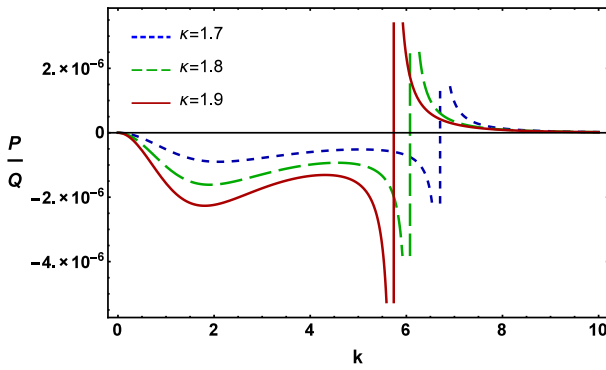


Figure 3: The variation of P/Q with k for different values of κ when other plasma parameters are $\rho = 1 \times 10^3$, $\mu = 3 \times 10^{-6}$, $\mu_2 = 0.3$, $\mu_3 = 0.05$, and $\omega \equiv \omega_f$.

where $\Phi = \phi_1^{(1)}$ for simplicity. In Eq. (38), the dispersion coefficients (P) and non-linear coefficients (Q) can be written, respectively, as

$$P = -\frac{(\omega - kv_g)(\omega^2 - \mu_2 k^2)^3 (3kv_g \mu_1 \mu_3 - \mu_1 \mu_2 \omega) + F_2}{\omega(\omega^2 - \mu_2 k^2)[2\mu_1 \mu_3 k^2 (\omega^2 - \mu_2 k^2)^2 + 2k^2 \omega^4]},$$

$$Q = \frac{\omega^3 (\omega^2 - \mu_2 k^2)^2 [3A_3 + 2A_2(A_8 + A_{13}) - F_3]}{2\mu_1 \mu_3 k^2 (\omega^2 - \mu_2 k^2)^2 + 2k^2 \omega^4},$$

where $F_2 = (2k\omega^6 v_g - 2\mu_2 k^2 \omega^5)(\omega - kv_g) + (\omega^4 kv_g - \omega^5)(\omega - kv_g)(\omega^2 + \mu_2 k^2) + \omega^4 (\omega^2 - \mu_2 k^2)^3$ and $F_3 = \{(k^2 \omega^2 + \mu_2 k^4)(A_7 + A_{12}) + 2k^3 \omega(A_6 + A_{11})\}/(\omega^2 - \mu_2 k^2)^2 + \{2k^3 \mu_1 \mu_3 (A_4 + A_9) + k^2 \omega \mu_1 \mu_3 (A_5 + A_{10})\}/\omega^3$. It is interesting that P and Q of the Eq. (38) are function of various plasma parameters such as carrier wave number (k), ratio of ion mass to dust mass (μ), ratio of dust charge state to ion charge state (ρ), and super-thermal parameter (κ), etc.

4. Modulational instability and rogue waves

The stable and unstable parametric regimes of the DIAWs are organized by the sign of the dispersion (P) and nonlinear (Q) coefficients of the standard NLSE [27, 28, 29]. The stability of DIAWs in a three-component DPM is governed by the sign of P and Q [27, 28, 29]. When P and Q have same sign

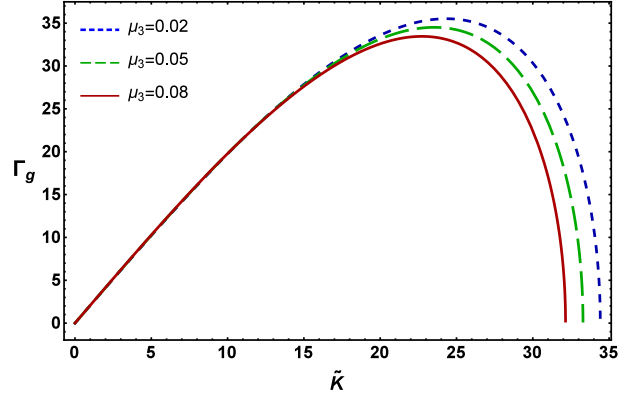


Figure 4: The variation of Γ_g with \tilde{k} for different values of μ_3 when other plasma parameters are $k = 1.0$, $\tilde{\Phi}_0 = 0.5$, $\kappa = 1.8$, $\rho = 1 \times 10^3$, $\mu = 3 \times 10^{-6}$, $\mu_2 = 0.3$, and $\omega \equiv \omega_f$.

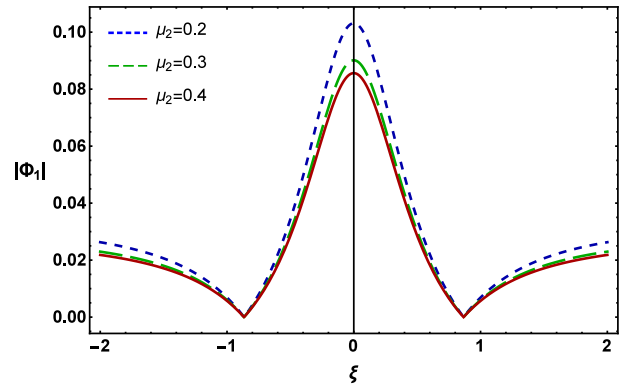


Figure 5: The variation of $|\Phi_1|$ with ξ for different values of μ_2 when other plasma parameters are $\tau = 0$, $k = 1.0$, $\tilde{\Phi}_0 = 0.5$, $\kappa = 1.8$, $\rho = 1 \times 10^3$, $\mu = 3 \times 10^{-6}$, $\mu_3 = 0.05$, and $\omega \equiv \omega_f$.

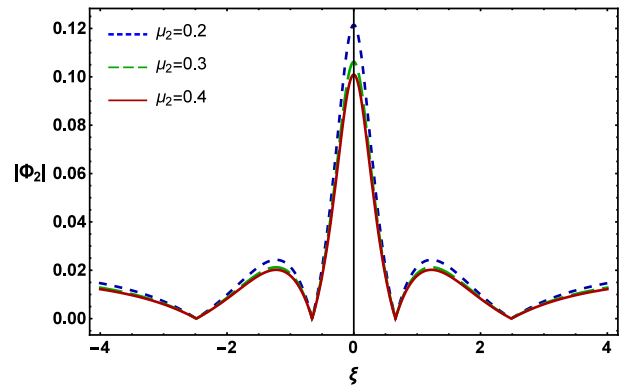


Figure 6: The variation of $|\Phi_2|$ with ξ for different values of μ_2 when other plasma parameters are $\tau = 0$, $k = 1.0$, $\tilde{\Phi}_0 = 0.5$, $\kappa = 1.8$, $\rho = 1 \times 10^3$, $\mu = 3 \times 10^{-6}$, $\mu_3 = 0.05$, and $\omega \equiv \omega_f$.

(i.e., $P/Q > 0$), the evolution of the DIAWs amplitude is modulationally unstable. On the other hand, when P and Q have opposite sign (i.e., $P/Q < 0$), the DIAWs are modulationally stable in the presence of external perturbations. The plot of P/Q against k yields stable and unstable parametric regimes of DIAWs. The point, at which transition of P/Q curve intersects with k -axis, is known as threshold or critical wave number k

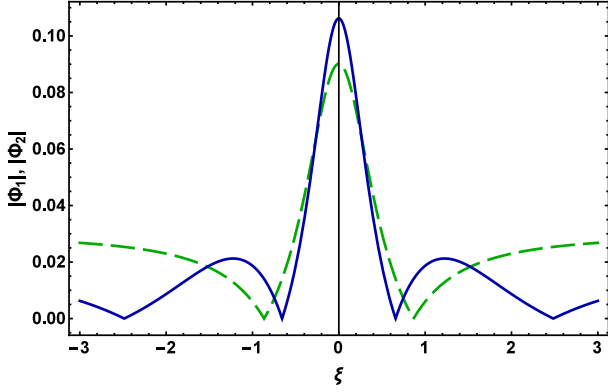


Figure 7: The variation of first-order (dashed green curve) and second-order (solid blue curve) rational solutions of NLSE at $k = 1.0$ and $\tau = 0$.

($= k_c$) [27, 28, 29, 30, 31, 32]. When $P/Q > 0$ and $\tilde{k} < k_c$, the MI growth rate (Γ_g) is given by

$$\Gamma_g = |P|\tilde{k}^2 \sqrt{\frac{\tilde{k}_c^2}{\tilde{k}^2} - 1}. \quad (39)$$

The first-order rational solution, which can predict the concentration of the large amount of energy in a small region in the modulationally unstable parametric regime ($P/Q > 0$) of DI-AWs, of Eq. (38) can be written as [33, 34]

$$\Phi_1(\xi, \tau) = \sqrt{\frac{2P}{Q}} \left[\frac{4 + 16i\tau P}{1 + 4\xi^2 + 16\tau^2 P^2} - 1 \right] \exp(2i\tau P). \quad (40)$$

and the second-order rational solution is

$$\Phi_2(\xi, \tau) = \sqrt{\frac{P}{Q}} \left[1 + \frac{G_2(\xi, \tau) + iM_2(\xi, \tau)}{D_2(\xi, \tau)} \right] \exp(i\tau P), \quad (41)$$

where

$$\begin{aligned} G_2(\xi, \tau) &= \frac{-\xi^4}{2} - 6(P\xi\tau)^2 - 10(P\tau)^4 \\ &\quad - \frac{3\xi^2}{2} - 9(P\tau)^2 + \frac{3}{8}, \\ M_2(\xi, \tau) &= -P\tau \left[\xi^4 + 4(P\xi\tau)^2 + 4(P\tau)^4 \right. \\ &\quad \left. - 3\xi^2 + 2(P\tau)^2 - \frac{15}{4} \right], \\ D_2(\xi, \tau) &= \frac{\xi^6}{12} + \frac{\xi^4(P\tau)^2}{2} + \xi^2(P\tau)^4 \\ &\quad + \frac{\xi^4}{8} + \frac{9(P\tau)^4}{2} - \frac{3(P\xi\tau)^2}{2} \\ &\quad + \frac{9\xi^2}{16} + \frac{33(P\tau)^2}{8} + \frac{3}{32}. \end{aligned}$$

The nonlinear behavior of the plasma medium is considered to be responsible for the concentration of large amount of energy into tiny region.

5. Results and discussion

First, we are interested to observe numerically the stable and unstable parametric regimes of DIAWs in the presence of super-thermal electrons by depicting the variation of P/Q with k for

different plasma parameters. In our present analysis, we have considered that $m_d = 10^6 m_i$, $Z_d = 10^3 Z_i$, and $T_e = 10 T_i$.

We have graphically shown the variation of P/Q with k in case of both fast (ω_f) and slow (ω_s) DIA modes for different values of κ in Figs. 2 and 3, respectively. From these two figures, it can be seen that (a) under consideration $\omega \equiv \omega_f$ and $\omega \equiv \omega_s$, possible stable and unstable parametric regimes can be occurred for DIAWs; (b) the DIAWs become unstable for small value of k (i.e., $k \approx 0.6$) in first mode while in slow mode the DIAWs become unstable for large value of k (i.e., $k \approx 6$) for same plasma parameters; and (c) the k_c decreases with an increase in the value of κ .

We have numerically analyzed the MI growth rate of DIAWs under consideration fast mode in Fig. 4 by using these plasma parameters: $k = 1.0$, $\tilde{\Phi}_0 = 0.5$, $\rho = 1 \times 10^3$, $\mu = 3 \times 10^{-6}$, and $\mu_2 = 0.3$. It is clear that the maximum value of the Γ_g increases (decreases) with the increase in the value of ion (dust) number density for a constant value of their charge state (via μ_3). The nonlinearity as well as the Γ_g increases (decreases) with ion (dust) charge state when other plasma parameters remain constant.

We have presented the evaluation of first and second-order DIARWs with ξ for different values of μ_2 in Figs. 5 and 6, respectively, and from these figures it is observed that both the first and second-order DIARW solutions can concentrate large amount of energy into a small region. It is clear from these two figures that (a) the amplitude of the first and second-order rogue waves decreases (increases) with increasing the temperature of the ion (electron) for a fixed ion charge state; (b) the nonlinearity as well as the amplitude and width of the first and second-order DIARWs increases with ion charge state.

Figure 7 shows a comparison between the first and second-order DIARWs and it can be seen from this figure that (a) the amplitude of the second-order DIARWs is always higher than the first-order DIARWs for same plasma parameters, which means that the second-order DIARWs can concentrate more energy than the first-order DIARWs; (b) the first-order DIARWs has two zeros symmetrically located on its ξ -axis, where the second-order DIARWs has four zeros symmetrically located on its ξ -axis.

6. Conclusion

In this paper, we have considered a realistic DPM having negatively charged dust grains, ions and electrons. A standard NLSE is derived by using RPM, and this three-component DPM can generate DIAWs in which the moment of inertia is provided by the warm ions and dust grains, and the restoring force is provided by the thermal pressure of inertialess super-thermal electrons. The interaction of the nonlinear (Q) and dispersive (P) coefficients of NLSE can easily divide the modulationally stable and unstable parametric regimes, and the unstable parametric regime also allows to generate highly energetic DIARWs. The outcomes of present investigation can be useful in explaining the DIARWs cometary tails [1, 2, 3, 4], magnetosphere [3], ionosphere [3], aerosols in the astrosphere [2], planetary rings [1], Earth's ionospheres [1], and interstellar medium [4].

References

- [1] P. Eslami, *et al.*, *IEEE Trans. Plasma Sci.* **41**, 3589 (2013).
- [2] N.S. Saini and K. Singh, *Phys. Plasmas* **23**, 103701 (2016).
- [3] M. Shahmansouri and M. Tribeche, *Astrophys. Space Sci.* **342**, 87 (2012).
- [4] P.K. Shukla and A.A. Mamun, *Introduction to Dusty Plasma Physics* (Institute of Physics, Bristol, 2002).
- [5] L. Boufendi, *et al.*, *Plasma Sources Sci. Technol.* **11**, 211 (2002).
- [6] T.S. Gill, *Phys. Plasmas* **17**, 013701 (2010).
- [7] M. Ferdousi and S. Sultana, *et al.*, *Eur. Phys. J. D* **71**, 102 (2017).
- [8] V.M. Vasyliunas, *J. Geophys. Res.* **73**, 2839 (1968).
- [9] M. Maksimovic, *J. Geophys. Res.* **105**, 18337 (2000).
- [10] V. Pierrad and M. Lazar, *Sol. Phys.* **267**, 153 (2010).
- [11] M.R. Amin, *Phys. Rev. E* **58**, 6517 (1998).
- [12] X. Jukui and L. He, *Phys. Plasmas* **10**, 339 (2003).
- [13] N.S. Saini and I. Kourakis, *Phys. Plasmas* **15**, 123701 (2008).
- [14] R. Fedele, *Phys. Scr.* **65**, 502 (2002).
- [15] N.A. Chowdhury, *et al.*, *Chaos* **27**, 093105 (2017).
- [16] N.A. Chowdhury, *et al.*, *Phys. plasmas* **24**, 113701 (2017).
- [17] M.H. Rahman, *et al.*, *Chinese J. Phys.* **56**, 2061 (2018).
- [18] M.H. Rahman, *et al.*, *Phys. Plasmas* **25**, 102118 (2018).
- [19] S.K. Paul, *et al.*, *Pramana-J Phys* **94**, 58 (2020).
- [20] N.A. Chowdhury, *et al.*, *Contrib. Plasma Phys.* **58**, 870 (2018).
- [21] N. Ahmed, *et al.*, *Chaos* **28**, 123107 (2018).
- [22] N.A. Chowdhury, *et al.*, *Plasma Phys. Rep.* **45**, 459 (2019).
- [23] S. Jahan, *et al.*, *Commun. Theor. Phys.* **71**, 327 (2019).
- [24] M. Hassan, *et al.*, *Commun. Theor. Phys.* **71**, 1017 (2019).
- [25] A.E. Dubinov, *Plasma Phys. Rep.* **35**, 991 **2009**.
- [26] E. Saberian, *et al.*, *Plasma Phys. Rep.* **43**, 83 (2017).
- [27] I. Kourakis and P.K. Shukla, *Phys. Plasmas* **10**, 3459 (2003).
- [28] I. Kourakis and P.K. Shukla, *Nonlinear Proc. Geophys.* **12**, 407 (2005).
- [29] N.A. Chowdhury, *et al.*, *Vacuum* **147**, 31 (2018).
- [30] R.K. Shikha, *et al.*, *Eur. Phys. J. D* **73**, 177 (2019).
- [31] T.I. Rajib, *et al.*, *Phys. plasmas* **26**, 123701 (2019).
- [32] S. Jahan, *et al.*, *Plasma Phys. Rep.* **46** (2020) 90.
- [33] A. Ankiewicz, *Phys. Lett. A* **373**, 3997 (2009).
- [34] S. Guo, *et al.*, *Ann. Phys.* **332**, 38 (2012).